The isolated flat silicon nanocrystals (2D structures) stabilized with perfluorophenyl ligands

A. S. Orekhov, S. V. Savilov, V. N. Zakharov, A. V. Yatsenko & L. A. Aslanov

Journal of Nanoparticle Research
An Interdisciplinary Forum for
Nanoscale Science and Technology

ISSN 1388-0764
Volume 16
Number 1

J Nanopart Res (2014) 16:1-8
DOI 10.1007/s11051-013-2190-4

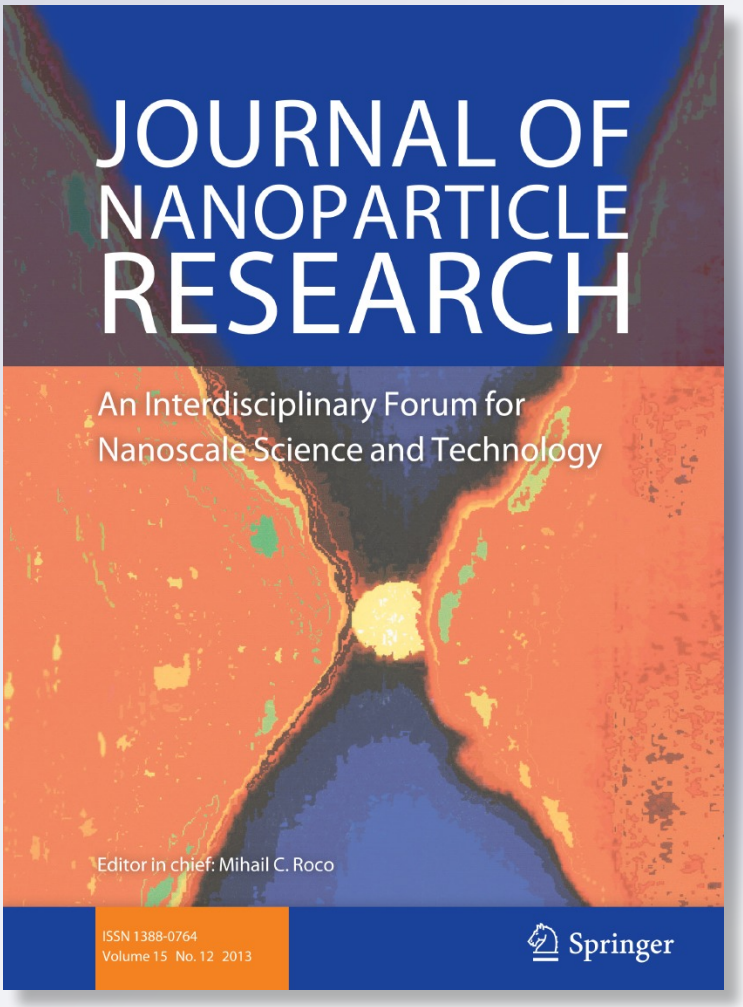

Springer

Your article is protected by copyright and all rights are held exclusively by Springer Science +Business Media Dordrecht. This e-offprint is for personal use only and shall not be self-archived in electronic repositories. If you wish to self-archive your article, please use the accepted manuscript version for posting on your own website. You may further deposit the accepted manuscript version in any repository, provided it is only made publicly available 12 months after official publication or later and provided acknowledgement is given to the original source of publication and a link is inserted to the published article on Springer's website. The link must be accompanied by the following text: "The final publication is available at link.springer.com".

Author's personal copy

J Nanopart Res (2014) 16:2190
DOI 10.1007/s11051-013-2190-4

BRIEF COMMUNICATION

The isolated flat silicon nanocrystals (2D structures) stabilized with perfluorophenyl ligands

A. S. Orekhov · S. V. Savilov · V. N. Zakharov · A. V. Yatsenko · L. A. Aslanov

Received: 8 July 2013 / Accepted: 30 November 2013
© Springer Science+Business Media Dordrecht 2013

Abstract Flat silicon nanocrystals coated with the perfluorophenyl ligands have been obtained. Flat silicon nanocrystals are formed due to specific interactions between the perfluorophenyl ligands. The fact of binding of the perfluorophenyl ligands to the surface of silicon nanoparticles is supported by XPS and FTIR spectroscopy. Morphology and structure of the synthesized Si-nanoparticles were studied using transmission electron microscopy. The samples comprise two types of nanoparticles: spherical and flat (2D structures). Electron diffraction pattern demonstrates that spherical Si-nanoparticles are amorphous. The spot diffraction patterns are observed for flat Si-nanoparticles which have the crystalline structure. The size of these particles varies from 15 to 50 nm. The thickness of flat nanocrystals was evaluated using atomic force microscopy; it appeared to be close to 3.3 nm in average. Small and large silicon nanoparticles are interrelated; large flat plates are the products of aggregation and crystallization of small nanoparticles. Nanocrystals exhibit photoluminescence with the emission maximum at 430 nm.

Keywords Silicon · Fluorinated ligands · Nanocrystals · 2D Structures · Photoluminescence · Crystal nanolayer

Introduction

Due to the unique optical and chemical properties, silicon nanocrystals (nc-Si) were prepared as quantum dots (Zou et al. 2004; Zhang et al. 2007; Sublemontier et al. 2009; Atkins et al. 2012; Gupta and Wiggers 2011; Dasog et al. 2013; Wang et al. 2013) or nanowire (Heitsch et al. 2008, Peng et al. 2013; He et al. 2011), but in the last 3–4 years, there appeared an interest to 2D structures (De Padova et al. 2010; Hoffmann 2013; Vogt et al. 2012; Kara et al. 2012; Lalmi et al. 2010; Jose and Datta 2011; Nakano et al. 2006; Wen et al. 2013; Son et al. 2009; Ithurria et al. 2011; Joo et al. 2006; Bouet et al. 2013; Ithurria and Dubertret 2008; Cassette et al. 2012; Tessier et al. 2012) produced on supports or in colloidal media. The 2D nanocrystals of semiconductors of $A^{II}B^{VI}$ type were obtained in the colloidal state; it was found that ligands play an important role in their growth (Wen et al. 2013; Son et al. 2009; Ithurria et al. 2011; Joo et al. 2006; Bouet et al. 2013; Ithurria and Dubertret 2008; Cassette et al. 2012; Tessier et al. 2012).

Electronic supplementary material The online version of this article (doi:10.1007/s11051-013-2190-4) contains supplementary material, which is available to authorized users.

A. S. Orekhov
Shubnikov Institute of Crystallography, RAS, Moscow, Russia

S. V. Savilov · V. N. Zakharov · A. V. Yatsenko · L. A. Aslanov (✉)
Department of Chemistry, Lomonosov Moscow State University, Moscow, Russia
e-mail: aslanov.38@mail.ru

Published online: 15 December 2013

Author's personal copy

The crystal dimensionality plays a major role in the nanostructure optical properties, e.g., ultrathin CdSe nanoribbons exhibit an extremely narrow photoluminescence band (Joo et al. 2006). The shape affects the strength of the exciton coupling with the emitted photons because the tangential component of the photon electric field does not change its value when it penetrates into one-dimensional or two-dimensional colloidal semiconductor structures. This in turn shortens the fluorescent decay time in these structures (Ithurria et al. 2011).

Recently, monoatomic silicon layers were extracted from the $CaSi_2$ crystals as they were and then stabilized by phenyl groups (Sugiyama et al. 2010) or hexyl groups (Nakano et al. 2012). The $CaSi_2$ crystals contain graphene-like layers consisting of Si atoms, and these layers are interlaced by Ca atoms. In the present study below, we describe assembling of the separate Si atoms into flat nanoparticles. It is stated that graphene-like monoatomic layers of silicon cannot be obtained without supports, that is, all 2D silicon structures prepared in colloidal media should have a certain thickness (Hoffmann 2013).

For the first time, we have obtained the sandwich-like flat nc-Si as freestanding crystals with the thickness less than 10 nm as a result of synthetic procedure in solution (bottom-up); the outer layers are formed by the perfluorophenyl ligands (Fig. 1), and flat silicon nanocrystal is located between two ligand layers. We have not observed such types of nanocrystals with other ligands, namely phenyl, carbene, alkyl, perfluorobutyl, and halide, synthesized under the same conditions as Si nanocrystals with perfluorophenyl ligands.

In contrast to flat crystals obtained by us, the grapheme-like monoatomic layers (Sugiyama et al. 2010) are not crystals but polymeric molecular formation.

Experimental section

Briefly, silicon nanoparticles were obtained by reduction of $SiBr_4$ ($SiCl_4$) with potassium in 1,2-dimethoxyethane, and the remaining bromide ligands on the nc-Si surface were replaced by perfluorophenyl groups on adding the nc-Si dispersion to the 20 % excess of perfluorophenyllithium prepared from bromopentafluorobenzene and lithium amalgam. Typical example of synthetic procedure and characterization methods are given in the Electronic Supplementary Material.

Results and discussion

The fact of binding of the perfluorophenyl ligands to the surface of silicon nanoparticles is supported by FTIR spectroscopy (Fig. 2); absorption bands at 1,459 and 1,243 cm^{-1} correspond with the Si–C bond oscillations (Shorafa et al. 2009; Sudeep et al. 2008), and broad peaks at 3,420 and 2,100 cm^{-1} correspond with the O–H and Si–H bond oscillations, respectively (Kelm et al. 2011; Ryabchikov et al. 2013). The presence of the O–H groups in large amounts is not surprising because of the electron-acceptor action of perfluorophenyl ligands promoting nucleophilic attack of atmospheric moisture on silicon nanoparticles. An intensive band at

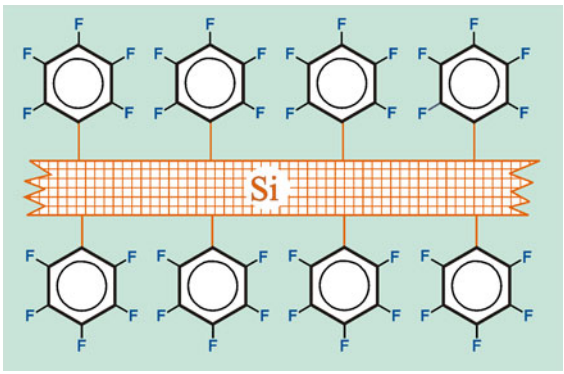

Fig. 1 Flat silicon nanocrystal stabilized by the perfluorophenyl ligands

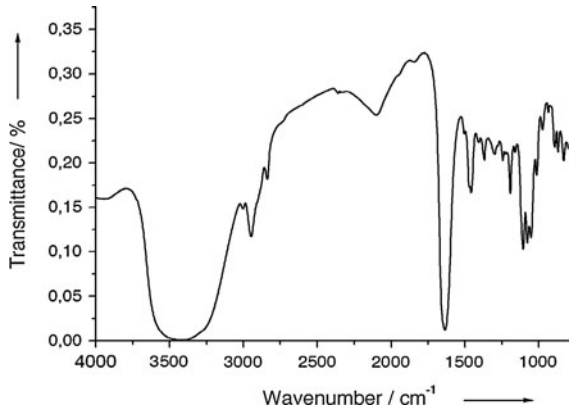

Fig. 2 FTIR spectrum of nanosilicon stabilized by the perfluorophenyl ligands

Author's personal copy

1,635 cm^{-1} has been attributed to Si–OH vibrations (Rao et al. 2011; Zheng et al. 2012; Xu et al. 2011; Fang et al. 2007). According to Ryabchikov et al. (2013), this band may indicate the presence of physically absorbed water molecules. However, heating of our nanosilicon samples to 350 °C under pressure 1,330 Pa for 3 h had no effect on FTIR spectrum, whereas the physically absorbed water should be removed mainly at 70 C (Peng et al. 2009), and its desorption is complete at 150 C (Zhuravlev, 2000). That is why we ruled out the presence of considerable amounts of the physically absorbed water in our samples.

An absorption band at 1,077 cm^{-1} can be attributed to the valence oscillations of the Si–O bond (Sudeep et al. 2008; Kelm et al. 2011). The valence oscillation peaks of the CH_2 groups at 2,947 and 2,838 cm^{-1} can be caused by octane used as a dispersion medium at the final stage of sample preparation.

In the FTIR spectra, the perfluorophenyl ligands gave absorption bands C–F 1,106 cm^{-1} (Woski et al. 2008; Inagaki et al. 1989), 1,052 cm^{-1} C=C–F (Sahin et al. 2006), 1,473 cm^{-1}, and 1,299 cm^{-1} −C=C− (Woski et al. 2008; Inagaki et al. 1989). The presence of Si–$C_{perfluorophenyl}$ bonds is also supported by XPS spectra (see Fig.S1, Fig.S2 in Supporting Information). A general XPS pattern is presented in Fig.S1. Concentrations of the elements observed on the surface of samples were calculated for the separate lines recorded for transmission energy 20 eV and appeared to be as follows: C 67.8, O 17.0, Si 11.0, F 3.2, Cl 0.9, and Hg < 0.1. The spectral line of Si 2p electrons in the studied samples is presented in Fig. S2. Two states of silicon stand out: the first one with the bond energy $\sim$ 102.5 eV is typical of organic Si-containing compounds, i.e., Si–$C_{perfluorophenyl}$ bond, and the second with bond energy more than 103.0 eV is typical of SiO_2.

Morphology and structure of the synthesized Si-nanoparticles were studied using Transmission Electron Microscopy (TEM). Samples were analyzed in the bright-field (BF TEM) mode and in the dark-field scanning mode (STEM, "Z-contrast").

The samples comprise two types of nanoparticles: spherical and flat (2D structures). TEM image of the spherical particles is presented in Fig. S3a. Spherical particles are uniformly distributed in the sample. Fig. S3b shows their size distribution plot. The average diameter of spherical particles is 4.0 ± 0.5 nm. Electron diffraction pattern (DP) demonstrates that spherical Si-nanoparticles are amorphous (Fig. S4, inset); only two diffuse rings are present in DP. This pattern is typical of amorphous material with the short-range order in atoms arrangement.

Along with halo-like DP from spherical particles, the spot diffraction patterns from some areas are observed for nanoparticles (Fig. 3a) which have the crystalline structure. The Energy Dispersive X-ray (EDX) analysis reveals the presence of C, Si, O and a trace amount of F (Fig. 3b). Small amount of oxygen in silicon nanoparticles could be captured during sample preparation for TEM investigation. The experimental DP is in a good agreement with the simulated diffraction pattern for cubic Si phase (space group Fd-3 m, $a = 0.543$ nm (Parrish 1960). It is important to note that in experimental DP, there are no 020 and 0-20 reflections forbidden in the space group Fd-3 m at [101] zone axis (International tables for X-ray crystallography 1996). Simulation of the dynamical selected area electron diffraction by JEMS program (Stadelmann 2012) shows that these reflections appear at crystal thickness above 10 nm (Fig. 3c). The intensity profiles of reflections along [010] direction clearly demonstrate that the specimen thickness is less than 10 nm; in Fig. 3d crystal thickness is 9 nm, and in Fig. 3e it is 10 nm. Thus, analysis of electron diffraction data indicates that thickness of these particles is less than 10 nm.

High-resolution TEM images of crystalline particles are shown in Figs. 4 and 5. The HRTEM images reveal a uniform contrast in the middle part of nanoparticle and a weak contrast near the edge (on the boundary of particle with support carbon film). The size of these particles can reach 50 nm. The reproducibility of particle dimensions was supported by six experiments. Thus, we can suppose that particles are rather thin ($d \leq 10$ nm) and form a flat 2D structure (Fig. 4). Fast Fourier transform (FFT) of the image corresponds to the silicon nanocrystal of cubic structure oriented by (101) plane normal to the electron beam (Fig. 4 insets). Attempts to index diffraction patterns on the hexagonal cell typical of silicene were unsuccessful.

The image calculation was performed for Si crystals with [101] and [112] zone axis (Fig. 5). A good agreement of the filtered experimental and simulated HRTEM images (insets) was found for the cubic Si phase with crystal thickness of 6.91 nm and defocus of 65.5 nm (Fig. 5a′) and for [112] crystal orientation with thickness of 9.31 nm and defocus of 64.5 nm (Fig. 5b′). Thickness values are within the previously evaluated range.

Author's personal copy

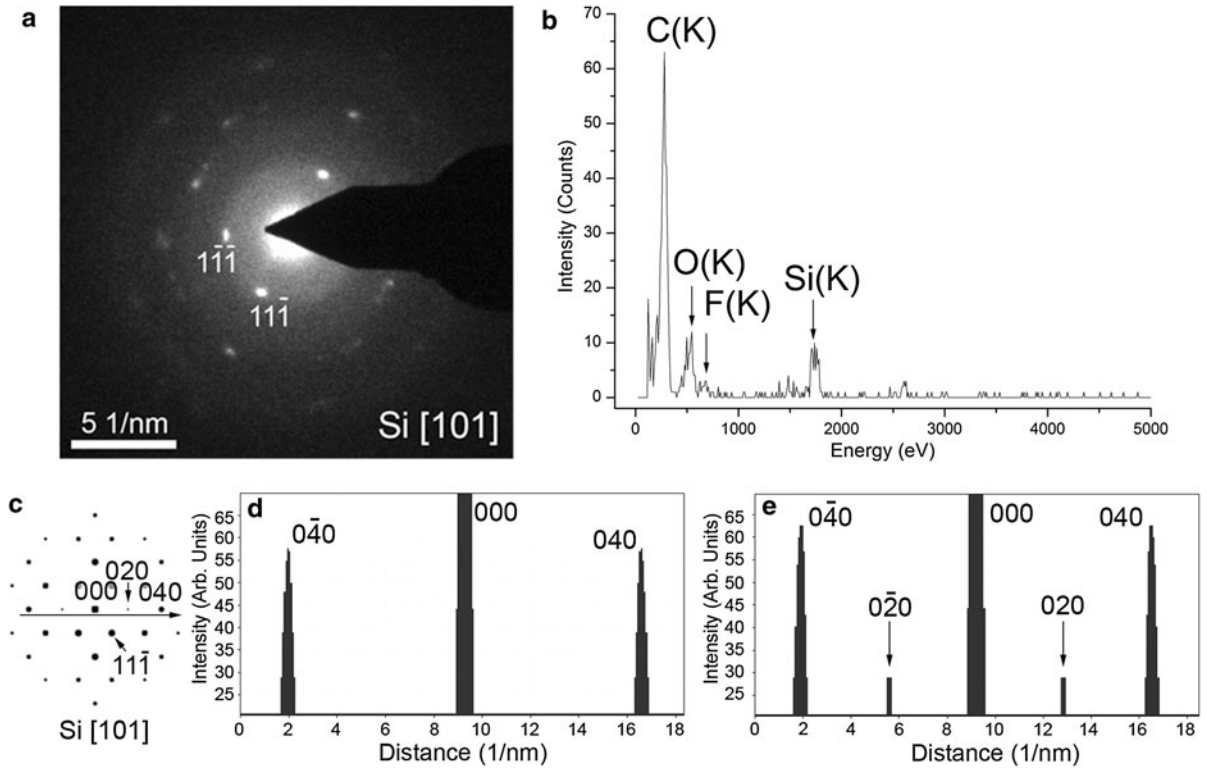

Fig. 3 Spot diffraction pattern indexed at [101] Si zone axis (**a**), EDX spectrum from crystalline particles (**b**), simulated dynamical selected area electron diffraction pattern (**c**) and intensity profiles of reflections along [010] direction for crystal thickness of 9 nm (**d**) and 10 nm (**e**), respectively

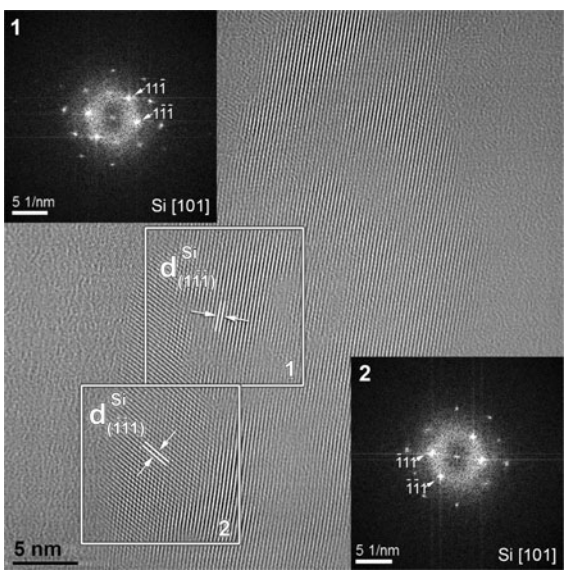

Fig. 4 Filtered HRTEM image of a large flat Si particle. *Insets* diffractograms of the isolated *squared areas* corresponding to [101] zone axis

The thickness of flat nanocrystals was evaluated using Atomic Force Microscopy (AFM) (Fig. S5); it appeared to be close to 3.3 nm in average, and areas of uniform thickness gained 30 nm on the support substrate. Thickness of flat silicon nanoparticls determined using AFM differs from that determined using TEM. This can be explained first, by the thickness distribution of nanoparticles and second, by poor TEM-image contrast and nonstability of thin nanoparticles due to a sufficient electron beam influence. The thicker nanosilicon plate, the higher is the contrast of TEM image and stability of nanosilicon plate in electron beam, that is why only images of nanoparticles with the maximal thickness were recorded. In contrast, random sampling of silicon nanoparticles was studied using AFM with thickness of flat nanoparticles significantly lower than the maximal one.

Since we performed a series of syntheses of nc-Si covered by phenyl, butyl, perfluorobutyl, and carbene ligands (Aslanov et al. 2010, 2013; Kamyshny et al.

Author's personal copy

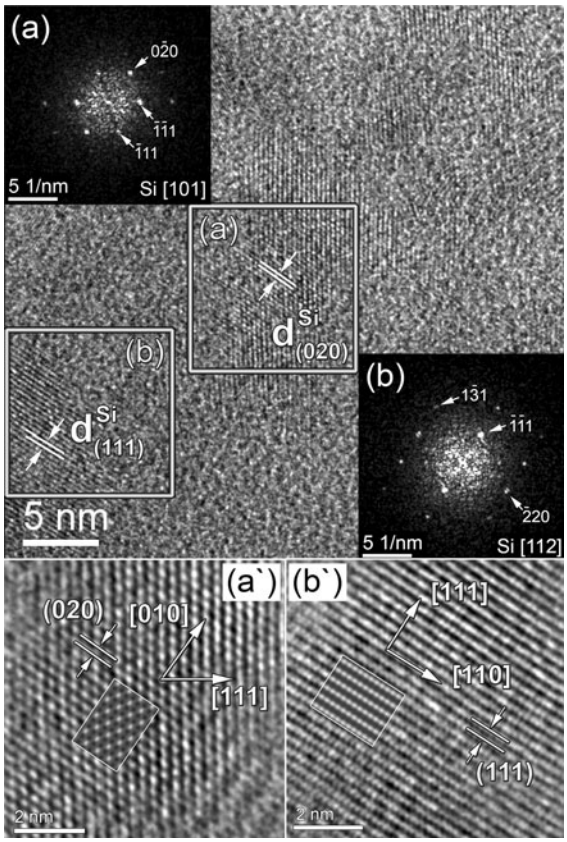

Fig. 5 HRTEM image of the flat Si crystals. *Insets* diffractograms of the isolated squared areas (*a*) and (*b*) corresponding to [101] and [112] zone axis, respectively. Image simulation (*insets*) shown on filtered image performed for two cases: defocus is 65.5 nm and assumed thickness 6.9 nm (*a*′); defocus is 64.5 nm and assumed thickness 9.3 nm (*b*′)

2011) using the same procedure, and in all of them only isotropic nanoparticles (quantum dots) were obtained, we have concluded that lamellar nanocrystals (Figs. 4, 5) are possibly formed at the stage of replacement of the bromide ligands by perfluorophenyl groups on the surface of small silicon nanoparticles and are the products of aggregation of these silicon nanoparticles in flat plates. In our opinion, growth of the plates is caused by C···F-specific interactions between the ligands, which results in formation of layers of the perfluorophenyl ligands due to their self-assembly in fluorophobic media. Small silicon nanoparticles are thus forced to aggregate in crystalline plates coated by perfluorophenyl ligands on both sides. So, small and large silicon nanoparticles are interrelated; large flat plates are the products of aggregation of small nanoparticles.

The mechanism of the perfluorophenyl ligand self-assembly is related with specific interactions. The centre of perfluorophenyl ring has a considerable positive charge because of attraction of electrons by fluorine atoms from π-orbitals of the perfluorophenyl ring, so the perfluorophenyl rings can interact with each other by a contact between the electronegative fluorine atom and the electropositive centre of perfluorinated ring (Reichenbächer et al. 2005); this is observed in the edge-to-face (T-shape) structure of hexafluorobenzene (Shiohara et al. 2010).

There are many examples of perfluorophenyl interactions via the offset face-to-face stacking between two C_6F_5 rings with short interplanar distances. In the cases where phenyl and perfluorophenyl groups coexist, the $C_6F_5\cdots C_6F_5$ stacking is unexpectedly observed rather than $C_6H_5\cdots C_6H_5$ one (Mountford et al. 2006; Sonoda et al. 2007; Liu et al. 2003; Blanchard et al. 2000; Bach et al. 2001; Han et al. 2011; Martin et al. 2008).

Along with the structure of pentafluorobenzoic acid (Han et al. 2011), two other crystal structures demonstrate the perfluorophenyl–perfluorophenyl interactions in the offset face-to-face mode but with different binding sites. The interplanar distances (3.30 and 3.23 Å) in these two crystal structures are close to the shortest intermolecular C···F distances. The data suggest that the C···F contacts occurring between the positive charge inside the perfluorophenyl ring and the negative charge on the fluorine atoms of the adjacent molecule are responsible for the perfluorophenyl–perfluorophenyl interaction. In the complex system, (Shiohara et al. 2010; Shorafa et al. 2009) the metal atoms play a role in further polarization of the highly polarized C–F bonds, and the $C_6F_5\cdots C_6F_5$ interactions are exceeded by the intermolecular C···F dipole–dipole interactions.

C_6F_5 ligands are bound to silicon atoms in the flat nc-Si particles which are under consideration. Presumably silicon atoms are able to impose extra polarization on C–F bonds like molybdenum and zinc atoms in coordination compounds (Han et al. 2011; Martin et al. 2008). It is noteworthy that the C···F contacts in the perfluorophenyl–perfluorophenyl pairs found in the structures described in (Han et al. 2011) are nearly perpendicular to the associated C–F bond direction. As was stated above, the C–F bond in the perfluorophenyl group has an anisotropic electron density distribution, i.e., the negative electrostatic potential for the side region but positive one for the

Author's personal copy

bond axial position, because the covalent C–F bond has a significant electrostatic contribution (O'Hagan 2008). The latter is considerably enhanced in the perfluorinated metal complex as mentioned above. Further polarization of the C–F bonds should lead to a relatively strong intermolecular dipole–dipole interaction. The normality of C···F contact to the C_6F_5 rings is indicative of the electrostatic donor–acceptor nature of the perfluorophenyl–perfluorophenyl interaction. The data suggest that the perfluorophenyl–perfluorophenyl interaction is essentially electrostatic and the aromatic π–π stacking makes negligible contribution in holding the crystal structure motifs.

In contrast to the perfluorophenyl, the perfluorobutyl ligands arrange silicon atoms in quantum dots but not in sheet-like aggregates (Aslanov et al. 2013) because of the absence of specific interactions C···F between perfluorobutyl ligands.

Nanosilicon which remains on glass support after evaporation of the solvent exhibits photoluminescence with the emission maximum at 430 nm (Fig. S6). Amorphous particles cannot luminesce due to the numerous broken bonds, and the perfluorophenyl ligands have a maximum in the UV region of the spectrum. For example, PL band in the spectrum of hexafluorobenzene lies in the range 300–470 nm with the maximum at 365 nm. The spectrum does not have any structure and is independent on λ_{ex} in the range 220–270 nm (Phillips 1967). That is why only the 2D nc-Si can luminesce by the action of the given λ_{ex}.

The 2D silicon nanocrystals as large as those presented in Fig. 3 can be doped for p-n junctions formation in con contrast to quantum dots in which the number of silicon atoms is ~ 1,000 whereas one boron or phosphorus dopant atom should be per 10^4 silicon atom.

Conclusion

The isolated flat silicon nanocrystals (2D structures) coated with perfluorophenyl ligands was obtained for the first time. Crystals were studied using FTIR, TEM, AFM, EDX, XPS, and PL spectroscopy. Flat silicon nanocrystals have been formed due to specific interactions between the perfluorophenyl ligands in fluorophobic media.

Acknowledgments The authors are grateful to V.V. Klechkovskaya for a valuable discussion and also to V.M. Senyavin, G.A. Shafeev, A.V. Simakin, and S.I. Gurskiy for their assistance in spectroscopic investigations. This study was financially supported by the Russian Foundation for Basic Research (grant no 11-03-01071), as well as by Lomonosov Moscow State University Program of Development.

References

Aslanov LA, Zakharov VN, Zakharov MA, Kamyshny AL, Magdassi Sh, Yatsenko AV (2010) Stabilization of silicon nanoparticles by carbenes. Russ J Coord Chem Pleiades Publishing Ltd 36:330–332

Aslanov LA, Zakharov VN, Pavlikov AV, Savilov SV, Timoshenko VYu, Yatsenko AV (2013) Synthesis and properties of nanosilicon stabilized by butyl and perfluorobutyl ligands. Russ J Coord Chem Pleiades Publishing Ltd 39:427–431

Atkins TM, Louie AY, Kauzlarich SM (2012) An efficient microwave-assisted synthesis method for the production of water soluble amine-terminated Si nanoparticles. Nanotechnology 23:294006/1–294006/9

Bach A, Lentz D, Luger P (2001) Charge Density and Topological Analysis of Pentafluorobenzoic Acid. J Phys Chem A 105:7405–7412

Blanchard D, Hughes RP, Concolino TE, Rheingold AL (2000) π-Stacking between Pentafluorophenyl and Phenyl Groups as a Controlling Feature of Intra- and Intermolecular Crystal Structure Motifs in Substituted Ferrocenes. Observation of Unexpected Face-to-Face Stacking between Pentafluorophenyl Rings. Chem Mater 12:1604–1610

Bouet C, Tessier MD, Ithurria S, Mahler B, Nadal B, Dubertret B (2013) Flat Colloidal Semiconductor Nanoplatelets. Chem Mater 25:1262–1271

Cassette E, Mahler B, Guigner J-M, Patriarche G, Dubertret B, Pons T (2012) Colloidal CdSe/CdS Dot-in-Plate Nanocrystals with 2D-Polarized Emission. ACS Nano 6:6741–6750

Dasog M, Yang Z, Regli S, Atkins TM, Faramus A, Singh MP, Muthuswamy E, Kauzlarich SM, Tilley RD, Veinot JGC (2013) Chemical Insight into the Origin of Red and Blue Photoluminescence Arising from Freestanding Silicon Nanocrystals. ACS Nano 7:2676–2685

De Padova P, Quaresima C, Ottaviani C, Sheverdyaeva PM, Moras P, Carbone C, Topwal D, Olivieri B, Kara A, Oughaddou H et al (2010) Evidence of graphene-like electronic signature in silicene nanoribbons. Appl Phys Lett 96:261905/1–261905/3

Fang J, Wang XF, Wang LS, Cheng B, Wu YT, Zhu W (2007) Preparation of modified SiO_2 colloidal spheres with succinic acid and the assembly of colloidal crystals. Chin Sci Bull 52:461–466

Gupta A, Wiggers H (2011) Freestanding silicon quantum dots: origin of red and blue luminescence. Nanotechnology 22:055707/1–055707/5

Han LJ, Fan LY, Meng M, Wang X, Liu CY (2011) Supramolecular assemblies of dimolybdenum transoids built by Mo2-enhanced perfluorophenyl–perfluorophenyl synthons. Dalton Trans 40:12832–12838

Author's personal copy

He Y, Zhong Y, Peng F, Wei X, Su Y, Su S, Gu W, Liao L, Lee S-T (2011) Highly Luminescent Water- Dispersible Silicon Nanowires for Long-Term Immunofluorescent Cellular Imaging. Angew Chem Int Ed 50:3080–3083

Heitsch AT, Fanfair DD, Tuan H-Y, Korgel BA (2008) Solution-liquid-solid (SLS) growth of silicon nanowires. J Am Chem Soc 130:5436–5437

Hoffmann R (2013) Small but Strong Lessons from Chemistry for Nanoscience. Angew Chem Int Ed 52:93–103

Hahn T (1996) International tables for X-ray crystallography, vol A. Kluwer, Dordreht

Inagaki N, Tasaka S, Kurita T (1989) Plasma polymerization of fluorobenzenes/sulfur dioxide mixtures. Polymer Bulletin (Berlin, Germany) 22:15–20

Ithurria S, Dubertret B (2008) Quasi 2D Colloidal CdSe Platelets with Thicknesses Controlled at the Atomic Level. J Am Chem Soc 130:16504–16505

Ithurria S, Tessier MD, Mahler B, Lobo RPSM, Dubertret B, Efros AL (2011) Colloidal nanoplatelets with two-dimensional electronic structure. Nat Mater 10:936–941

Joo J, Son JS, Kwon SG, Yu JH, Hyeon T (2006) Low-Temperature Solution-Phase Synthesis of Quantum Well Structured CdSe Nanoribbons. J Am Chem Soc 128:5632–5633

Jose D, Datta A (2011) Structures and electronic properties of silicene clusters: a promising material for FET and hydrogen storage. Phys Chem Chem Phys 13:7304–7311

Kamyshny A, Zakharov VN, Zakharov MA, Yatsenko AV, Savilov SV, Aslanov LA, Magdassi S (2011) Photoluminescent silicon nanocrystals stabilized by ionic liquid. J Nanopart Res 13:1971–1978

Kara A, Enriquez H, Seitsonen AP, Lew Yan Voon LC, Vizzini S, Aufray B, Oughaddou H, Kelm E, Korovin S, Pustovoy V, Surkov A, Vladimirov A (2012) A review on silicene—new candidate for electronics. Surf Sci Rep 67:1–18

Kelm E, Korovin S, Pustovoy V, Surkov A, Vladimirov A (2011) Luminescent silicon nanoparticles with magnetic properties—production and investigation. Appl Phys B: Lasers and Optics 105:599–606

Lalmi B, Oughaddou H, Enriquez H, Kara A, Vizzini S, Ealet B, Aufray B (2010) Epitaxial growth of a silicone sheet. Appl Phys Lett 97:223109/1–223109/2

Liu J, Murray EM, Young VG Jr (2003) π-Stacking interactions in some crystalline cisoid E, E-1,4-diaryl-1,3-butadienes. Chem Comm 15:1904–1905

Martin E, Spendley C, Mountford AJ, Coles SJ, Horton PN, Hughes DL, Hursthouse MB, Lancaster SJ (2008) Synthesis, Structure, and Supramolecular Architecture of Benzonitrile and Pyridine Adducts of Bis(pentafluorophenyl)zinc: pentafluorophenyl-Aryl Interactions versus Homoaromatic Pairing. Organometallics 27:1436–1446

Mountford AJ, Lancaster SJ, Coles SJ, Horton PN, Hughes DL, Hursthouse MB, Light ME (2006) The Synthesis, Molecular Structures, and Supramolecular Architecture of Amine Adducts of Bis(pentafluorophenyl)zinc. Organometallics 25:3837–3847

Nakano H, Mitsuoka T, Harada M, Horibuchi K, Nozaki H, Takahashi N, Nonaka T, Seno Y, Nakamura H (2006) Soft synthesis of single-crystal silicon monolayer sheets. Angew Chem Int Ed 45:6303–6306

Nakano H, Nakano M, Nakanishi K, Tanaka D, Sugiyama Y, Ikuno T, Okamoto H, Ohta T (2012) Preparation of alkyl-modified silicon nanosheets by hydrosilylation of layered polysilane (Si_6H_6). J Am Chem Soc 134:5452–5455

O'Hagan D (2008) Understanding organofluorine chemistry. An introduction to the C-F bond. Chem Soc Rev 37:308–319

Parrish W (1960) Results of the IUCr precision lattice-parameter project. Acta Cryst. 13:838–850

Peng L, Qisui W, Xi L, Chaocan Zh (2009) Investigation of the states of water and OH groups on the surface of silica. Colloids and Surfaces A: physicochem. Eng. Aspects 334:112–115

Peng F, Su Y, Wei X, Lu Y, Zhou Y, Zhong Y, Lee S-T, He Y (2013) Silicon-Nanowire-Based Nanocarriers with Ultra-high Drug-Loading Capacity for In Vitro and In Vivo Cancer Therapy. Angew Chem Int Ed 52:1457–1461

Phillips D (1967) Fluorescence and triplet state of hexafluorobenzene. J Chem Phys 46:4679–4689

Rao AV, Latthe SS, Kappenstein C, Ganesan V, Rath MC, Sawant SN (2011) Wetting behavior of high energy electron irradiated porous superhydrophobic silica films. Appl Surf Sci 257:3027–3032

Reichenbächer K, Süss HI, Hulliger J (2005) Fluorine in crystal engineering—"the little atom that could". Chem Soc Rev 34:22–30

Ryabchikov YV, Alekseev SA, Lysenko V, Bremond G, Bluet J-M (2013) Photoluminescence of silicon nanoparticles chemically modified by alkyl groups and dispersed in low-polar liquids. J Nanopart Res 15:1535–1543

Sahin E, Sahmetlioglu E, Akhmedov IM, Tanyeli C, Toppare L (2006) Synthesis and characterization of a new soluble conducting polymer and its electrochromic devices. Org Electron 7:351–362

Shiohara A, Hanada S, Prabakar S, Fujioka K, Lim TH, Yamamoto K, Northcote PT, Tilley RD (2010) Chemical Reactions on Surface Molecules Attached to Silicon Quantum Dots. J Am Chem Soc 132:248–253

Shorafa H, Mollenhauer D, Paulus B, Seppelt K (2009) The Two Structures of the Hexafluorobenzene Radical Cation C6F6.+. Angew Chem Int Ed 48:5845–5847

Son JS, Wen X-D, Joo J, Chae J, Baek S, Park K, Kim JH, An K, Yu JH, Kwon SG et al (2009) Large-Scale Soft Colloidal Template Synthesis of 1.4 nm Thick CdSe Nanosheets. Angew Chem Int Ed 48:6861–6864

Sonoda Y, Goto M, Tsuzuki S, Tamaoki N (2007) Fluorinated Diphenylpolyenes: crystal Structures and Emission Properties. J Phys Chem A 111:13441–13451

Stadelmann P (2012) The Java Electron Microscopy Software (JEMS). http://cimewww.epfl.ch

Sublemontier O, Lacour F, Leconte Y, Herlin-Boime N, Reynaud C (2009) CO2 laser-driven pyrolysis synthesis of silicon nanocrystals and applications. J All Comp 483:499–502

Sudeep PK, Page Z, Emrick T (2008) PEGylated silicon nanoparticles: synthesis and characterization. Chem Comm 46:6126–6127

Sugiyama Y, Okamoto H, Mitsuoka T, Morikawa T, Nakanishi K, Ohta T, Nakano H (2010) Synthesis and optical properties of monolayer organosilicon nanosheets. J Am Chem Soc 132:5946–5947

Author's personal copy

Tessier MD, Javaux C, Maksimovic I, Loriette V, Dubertret B (2012) Spectroscopy of Single CdSe Nanoplatelets. ACS Nano 6:6751–6758

Vogt P, De Padova P, Quaresima C, Avila J, Frantzeskakis E, Asensio MC, Resta A, Ealet B, Le Lay G (2012) Silicene: compelling experimental evidence for graphenelike two-dimensional silicon. Phys Rev Lett 108:155501/1–155501/5

Wang J, Ganguly S, Sen S, Browning ND, Kauzlarich SM (2013) Synthesis and characterization of P-doped amorphous and nanocrystalline Si. Polyhedron 58:156–161

Wen X-D, Hoffmann R, Ashcroft NW (2013) Two-Dimensional CdSe Nanosheets and their Interaction with Stabilizing Ligands. Adv Mater 25:261–266

Woski M, Berger RJF, Mitzel NW (2008) On the presence or absence of geminal Si···N interactions (α-effect) in pentafluorophenylsilyl compounds with SiCN, SiNN and SiON backbones. Dalton Trans 41:5652–5658

Xu G-L, Deng L–L, Pi P-H, Wen X-F, Zhen D-F, Cai Z-Q, Chen Q, Yang Zh-R (2011) Preparation and Characterization of Superhydrophobic/Superoleophilic SiO_2 Film. Integrated Ferroelectrics 127:9–14

Zhang X, Neiner D, Wang S, Louie AY, Kauzlarich SM (2007) A new solution route to hydrogen-terminated silicon nanoparticles: synthesis, functionalization and water stability. Nanotechnology 18:095601/1–095601/6. doi:10.1088/0957-4484/18/9/095601

Zheng G, Cui X, Zhang W, Tong Zh, Li F (2012) Preparation of nano-sized Al2O3–2SiO2 powder by sol–gel plus azeotropic distillation method. Particuology 10:42–45

Zhuravlev LT (2000) The surface chemistry of amorphous silica. Zhuravlev model. Colloids Surf A: Physicochem and Eng Aspects 173:1–38

Zou J, Baldwin RK, Pettigrew KA, Kauzlarich SM (2004) Solution Synthesis of Ultrastable Luminescent Siloxane-Coated Silicon Nanoparticles. Nano Lett 4:1181–1186